Nationaal Lucht- en Ruimtevaartlaboratorium

National Aerospace Laboratory NLR

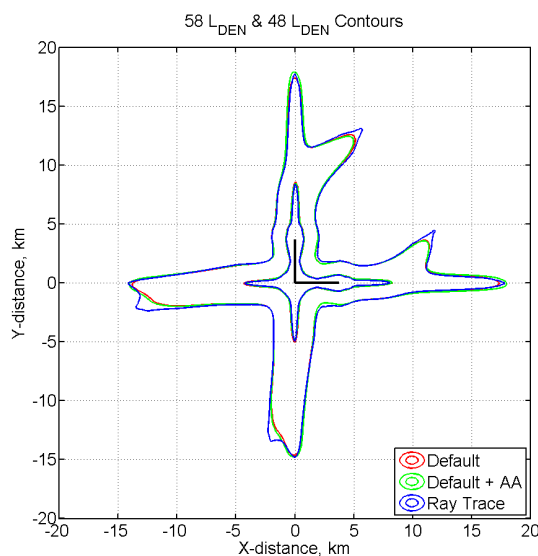## Executive summary

A weather dependent noise contour prediction concept

Calculating multi-event noise contours with ray-tracing

58 L_{DEN} & 48 L_{DEN} Contours

Problem area

The most frequently used excess attenuation method for noise contour models is called the lateral attenuation correction and this empirical method disregards varying atmospheric conditions. However, it is known that for single-event cases varying atmospheric conditions can lead to large discrepancies in results. The lateral attenuation is for instance used in both the Integrated Noise Model (INM) and the European calculation method as prescribed by ECAC Doc.29. The question remains how accurate the model is to predict the yearly noise contours when using this standardized method for multi-event cases. Also the distinct effect of particular atmospheric parameters on the noise contours is not clearly understood.

Description of work

To examine the atmospheric effects on the yearly contours, an advanced noise model is used to calculate the noise load around a fictive airport. The airport is comparable to a regional size airport and therefore an appropriate regional aircraft is used for this study. The weather is taken from the meteorological station "de Bilt" and is therefore representative for the Dutch situation. The advanced noise model that has been used is the NLR implementation of Doc.29

where the lateral attenuation correction can be replaced by a ray tracing prediction. This theoretical ray tracing model takes wind, temperature and humidity effects explicitly into account. Consequently it is now possible to calculate yearly noise contours using the default lateral attenuation method, the absorption corrected default method and the ray tracing method.

Results and conclusions
The yearly contour indicates that the results of the default and default method corrected for absorption are similar compared to the ray tracing prediction. For the long term average, the wind does not have a dramatic influence as reported earlier this year for single-events. In general, when taking the variation per month into account, it is concluded that the varying atmospheric absorption over the ray path has the most influence. This

effect becomes more pronounced for take-off procedures since the altitude of the aircraft is flying higher compared to an approach procedure. Overall differences in contour area are reported but shown to be directly related to absorption and/or the ground attenuation. Wind effects are, for the 48 L_{DEN} contour, 1 order of magnitude smaller. For the 58 L_{DEN} contour wind does not seem to play a significant role.

Applicability
The results and conclusions apply to the Dutch situation, given the atmospheric data, for multiple events only. For single-events, large differences due to the wind can occur. The noise model itself is generic meaning that different airport layouts, procedures or atmospheric data can be used to study local atmospheric dependent noise contours.

NLR-TP-2012-422

A weather dependent noise contour prediction concept

Calculating multi-event noise contours with ray-tracing
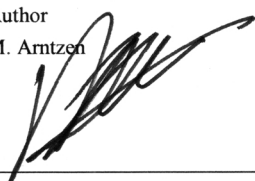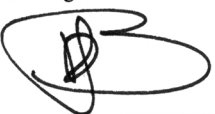
M. Arntzen, S.J. Heblij and D.G. Simons[1]

[1] TU Delft

Customer	National Aerospace Laboratory NLR
Contract number	4003105.1
Owner	NLR
Division NLR	Air Transport
Distribution	Unlimited
Classification of title	Unclassified
	October 2012

Approved by:

Author M. Arntzen	Reviewer Dick Bergmans	Managing department Roland Vercammen
Date: 08-10-12	Date: 08-10-2012	Date: 8-10-2012

Contents

This page is intentionally left blank.

A weather dependent noise contour prediction concept: Calculating multi-event noise contours with ray-tracing

Michael Arntzen[1] and Sander J. Heblij[2]
National Aerospace Laboratory (NLR), 1059 CM, Amsterdam, the Netherlands

Dick G. Simons[3]
TU Delft, 2629 HS, Delft, the Netherlands

This paper expands recent work on a standard aircraft noise model with an advanced excess attenuation method. The most frequently used excess attenuation method for noise contour models is called the lateral attenuation correction and this empirical method disregards varying atmospheric conditions. However, it is known that for single-event cases varying atmospheric conditions can lead to large discrepancies in results. This paper studies these effects for a longer period, involving multi-event calculations. An ECAC Doc.29 compliant noise model is utilized which is extended with the functionality to apply results from a ray tracing excess attenuation calculation. Results are shown for monthly and yearly noise contours around a fictive airport using different modeling options. In the end the differences in results between the three modeling options are small. However, some differences can be distinguished for both the 58 L_{DEN} and 48 L_{DEN} contour. The most prominent difference is a smaller 58 L_{DEN} contour area and a larger 48 L_{DEN} contour area. Based on the results, it is argued that the effects of refraction, ground attenuation and atmospheric absorption each play a distinctive role in the found differences. In conclusion, the lateral attenuation model, used to estimate the average excess attenuation in a varying atmosphere, provides a practical and realistic estimate for a yearly and monthly noise contour.

Nomenclature

L_{DN}	=	day-night level
L_{DEN}	=	day-evening-night level
N	=	number of flight operations
N_e	=	number of effective flights
Q	=	plane-wave reflection coefficient
T	=	traffic load
Z	=	normalized ground impedance
i	=	selected route
Γ	=	period-of-day multiplier for L_{DEN}
θ	=	incidence angle of acoustic ray

I.   Introduction

AIRPORTS are continuously confronted to deal with the impact of aircraft noise on the quality of life in the surrounding communities. Especially given the fact that the amount of traffic is still expected to increase all over the world in the next decennia, according to both major aircraft manufacturers.[1,2] Accordingly, policies are made to deal with the growing number of aircraft and airport operations. Predictions of aircraft noise play a large

---

[1] PhD Candidate, Environment and Policy Support, Anthony Fokkerweg 2.
[2] Research Engineer, Environment and Policy Support, Anthony Fokkerweg 2.
[3] Full Professor, Air Transport & Operations, Kluyverweg 1.

role in the policy making process and resulting regulations. These regulations are usually based on noise contours expressed in yearly averaged metrics like the L_{DEN} (Europe) or L_{DN} (USA).

It is well known that current predictive noise models like INM[3] and the procedure prescribed by Doc.29[4, 5] can be improved.[6,7] INM is the FAA's official method to calculate the noise impact. The European Civil Aviation Conference (ECAC) proposes a similar method (using identical equations) in their Document 29. These noise models use Noise-Power-Distance (NPD) information as the back-bone of the modeling effort. An NPD relation, usually tabulated, gives the resulting sound level at a distance, at a microphone height of 1.2 meter, as a function of the aircrafts thrust level. This NPD information is used in conjunction with standard noise calculation methods and typically based on aircraft manufacturer's data. The NPD based models are relatively fast, which is desirable for contour calculations since these may involve a lot of grid points and flights operations. The same holds for optimization studies were the number of noise model runs is high.

Since NPD data aims to include the sound level at several distances, basic attenuation of the sound over distances is inherently present in the data. This basic attenuation constitutes to spherical spreading losses and atmospheric absorption defined by a standard atmosphere.

NPD data is typically obtained after measurement of an aircraft under certification-like conditions and averaging of the noise results. In order to account for further propagation effects such as refraction and absorption by the ground surface, frequent use is made of a Lateral Attenuation (LA) correction.[8] The LA correction is based on a function which provides an estimate of the attenuation to the side of the aircraft in excess of the standard NPD attenuation. A semi-empirical standard function for the LA is used as a default in most NPD based models to correct for these factors.

It is well known that atmospheric propagation effects have a significant impact on the received noise on the ground.[9-12] When single-events are considered, the averaging of the NPD data, atmospheric absorption and utilization of the standardized LA correction method might lead to large differences due to the actual weather conditions. In case of noise maps calculated for an entire year these cumulative, or multi event, differences have not been studied extensively. The underlying LA correction function is based on a trend found by averaging measured Excess Attenuation (EA) throughout a long period. The correction function thus implicitly assumes that the average EA is adequately modeled when using the LA correction for a yearly contour. However, regulations for airports are usually based on such studies. Since the atmosphere is changing on a daily basis and can be different from the average EA correction method, differences in noise contours can occur. As a result, the influence of the varying atmosphere on annual noise contours around airports is not definitely answered in our opinion. More specifically the following questions are studied:

- What is the influence of varying weather on the L_{DEN} contours around an airport?
- Does the standard LA correction method provide a representative average for the varying atmospheric conditions on a yearly basis?

With help of this study, an answer is sought that may further validate the use of the default empirical (LA) correction method for multi-event calculations. Although the study is as generic as possible, the atmospheric data, and therefore the results are, at least to some extent, illustrative to the Dutch situation.

II. Study setup

A. Noise model

The computational method is based on ECAC Doc.29. The Doc.29 doctrine is augmented by a ray tracing algorithm.[9] Ray tracing is a well-established technique to calculate atmospheric propagation effects on noise.[10-12] The technique, and a typical result for a single-event, is briefly described in the next section. At this stage, the role of the ray tracing algorithm in the Doc.29 doctrine is described.

In the current implementation, the ray tracing algorithm effectively pre-computes the actual EA based on atmospheric data specified by the user. By using this tool the actual EA as influenced by the atmosphere is used rather than a default empirical function. Figure 1 shows the relation between the EA generator (ray tracing algorithm) and the noise model.

By using the approach depicted in Figure 1 it is possible to separate the more computational demanding EA generation from the actual contour calculation algorithm. Once the EA database is generated for a particular (stratified) atmosphere, the results can be reused for the calculation of different airport layouts or routes. As a result, the computational efficiency of the original NPD based noise model is left intact. The computational expense is only slightly increased due to input-output operations associated with including the EA database. But on an overall level, the runtime is similar to the default empirical functions.
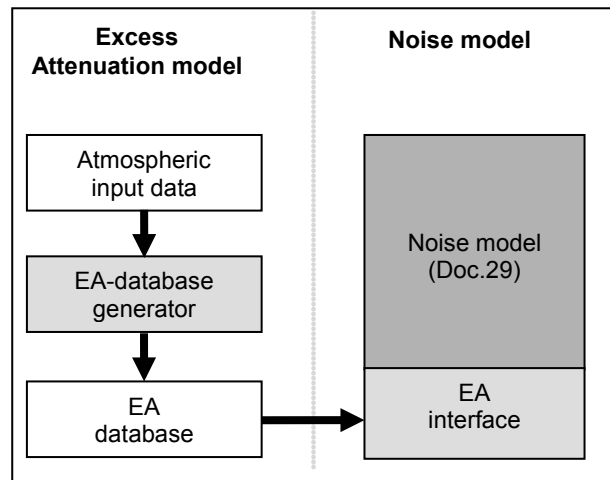

Figure 1. **The methodology used to correct the noise model.**

B. Generating the Excess Attenuation database

The atmospheric attenuation is caused by three elements: spreading of sound, atmospheric absorption and ground reflection. If atmospheric effects like varying wind and temperature are ignored, an element on the acoustic wave front travels along a straight acoustic ray path (classical straight line assumption) from the source towards the receiver. The wave front, from a point source, thus expands as a sphere. The resulting propagation losses due to spreading used in many noise models is referred to as spherical spreading losses.

The noise model should be supplied with the attenuation in excess of the attenuation that is already included in the NPD data. This calculation procedure of the EA database is laid down in Figure 2.
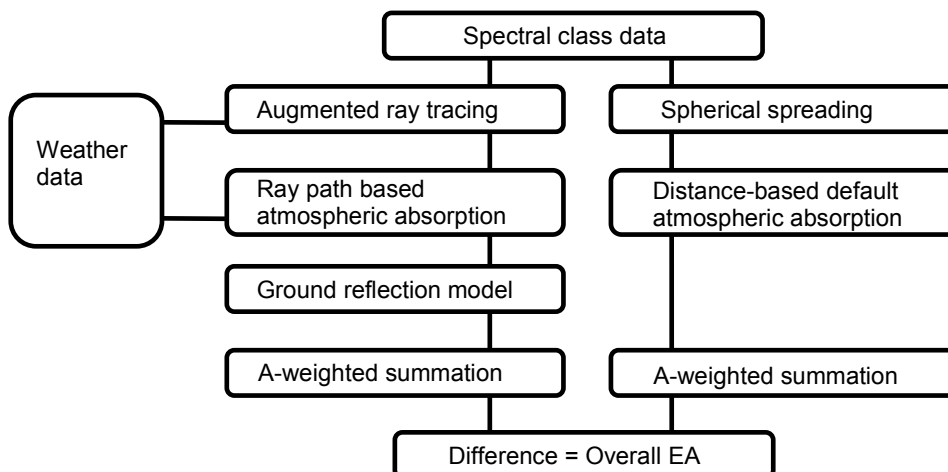

Figure 2.   **The procedure to calculate the Excess Attenuation database.**

The difference in EA, resulting from the calculation depicted in Figure 2, is thus based on the overall difference caused by the three attenuation mechanisms. These mechanisms are described briefly in the following paragraphs.

Due to wind and temperature gradients sound refracts, i.e. the ray path curvs.[13, 14] Using spreading losses predicted by the standard straight line method for varying atmospheric conditions is incorrect from a theoretical viewpoint. With the help of ray tracing based on the numerical integration of Snell's law of refraction[15], the actually curved paths can be found and the associated spreading losses are calculated. Two theoretical limitations of ray

tracing, i.e. shadow zones and caustics, are treated by using a high fidelity calculation method that is referred to as a Fast Field Program (FFP).[16] Typical results for such limiting conditions are found for combinations of the temperature and wind gradients with the FFP. These results are used to formulate an empirical law, for the shadow zone, and to limit the sound pressure predicted by a caustic. As a result, the results of the ray tracing calculation are augmented by observations based on a high fidelity tool. These results were presented and shown to be adequate for this papers implementation.[9, 10]

During a flyover the direct ray and a ground reflected ray arrive at a grid position with a phase difference. As a result, a ground interference pattern occurs in the sound spectrum. This interference pattern materializes as a decrease and increase in sound level at specific frequencies which varies with aircraft position. Since a segmented approach is used in standardized NPD based noise models, applying an interference pattern at discrete aircraft positions, i.e. using specific phase differences, will cause wrong results. Therefore, the phase differences were neglected but the attenuation of the ground was taken into account. This effectively constitutes to taking the incoherent effect on the ground attenuation into account as: [14]

$$\Delta SPL = 20 \cdot \log_{10}\left(\frac{1}{|Q|}\right) \tag{1}$$

were Q is the plane wave reflection coefficient defined by:

$$Q = \frac{Z \sin(\theta) - 1}{Z \sin(\theta) + 1} \tag{2}$$

and θ is the incidence angle of the acoustic ray with respect to the ground and Z is the normalized ground impedance as given by the (one-parameter) Delaney and Bazley model.[17] The ground surface is defined as a grass covered surface with an effective flow resistivity (σ_e = 250 kPasm^{-2}). With help of this single parameter the normalized ground impedance (Z) can be calculated by the model proposed by Delaney and Bazley.

To correct for the ground reflection inherently present in the NPD tables, measured at a flyover angle of 90 degrees w.r.t. the grass ground surface, the result at 90 degrees is subtracted. Consequently, there is no contribution to the overall attenuation of the ground model when the aircraft is exactly overhead. Only at angles other than 90 degrees, the ground model adds to the attenuation of the sound level. Ignoring the phase difference (for all angles of incidence) is judged to be reasonable approach since, for a continuous flyover, the interference pattern is changing constantly. Changes in interference pattern due to the wind, for flyover conditions, can be ignored as the effect on typical noise metrics is small.[10]

The atmosphere absorbs a sound wave as it passes through the medium. NPD tables, and therefore the default Doc.29 algorithm, include atmospheric absorption as calculated for a standard condition.[18] For varying atmospheric conditions a modification of the absorption effect can be used. This correction, based on a standardized method[19], uses the humidity and temperature on the ground to calculate the actual absorption rates. Such an assumption leads to applying uniform absorption conditions over the classical straight ray path. The augmented ray tracing uses the same standardized method but calculates the local, varying, atmospheric absorption conditions. As a result, a non-uniform atmospheric absorption is accumulated over a curved path and taken into account. These differences are addressed in the discussion section as they play a prominent role.

To demonstrate typical differences between the default and the augmented ray trace solution, a single-event result is included in Figure 3.[9] In this particular case, the aircraft is flying in the middle of the grid on a small segment heading towards the East.
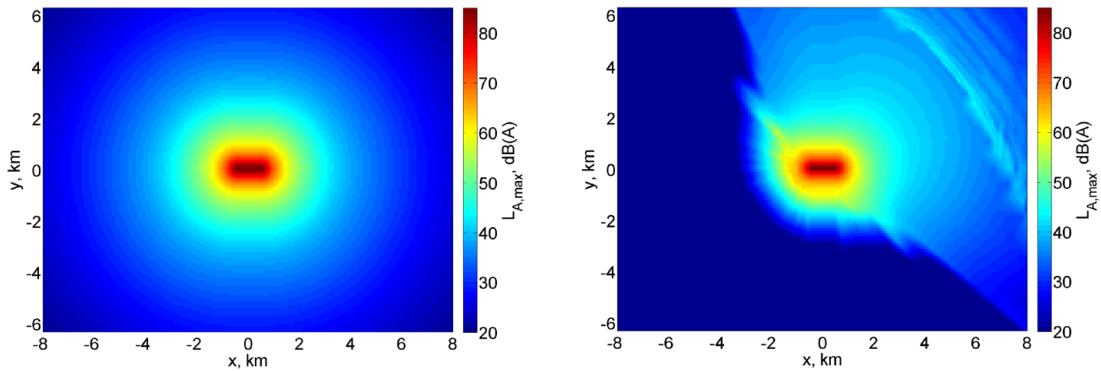
Figure 3. **Two footprints for a small segment of a flight trajectory (single-event). Left shows the default solution as calculated by the Doc.29 compliant noise model, right shows the solution including the augmented ray tracing results.**

As shown in Figure 3, the default solution differs severely from the solution based on ray tracing. A striking asymmetry between the South-West and North-East of the grid is present and can be related to the prevailing South-West wind direction. To the North-East of the aircraft, the sound level increases at a specific distance due to the fact that sound rays are curved downwards.

C. Airport layout and considered aircraft

For the multi-event case, treated in this paper, traffic around a fictive airport is modeled. The fictive airport is equipped with one runway in North-South direction and one in East-West direction. On every runway a standardized approach and departure route is defined. A route is selected depending on the wind direction on the ground since aircraft are bound to take-off and approach with headwind. For a considered wind direction only one runway will accommodate all approaching and departing traffic. For example runway 36 (heading 360 / heading North) is selected for departures and approaches if the wind is coming from the North. The actual wind direction stems from the atmospheric data and is sorted to come from the North, East, South or West for runway selection.

To model dispersion around a main route, as is common practice in noise modeling, sub routes are defined to the left and right of the main route. The majority of aircraft (60%) is flown over the main route whereas the two sub-routes each accommodate a traffic load of 20%. Figure 4 shows the departure and approach routes and the dispersion trajectories.
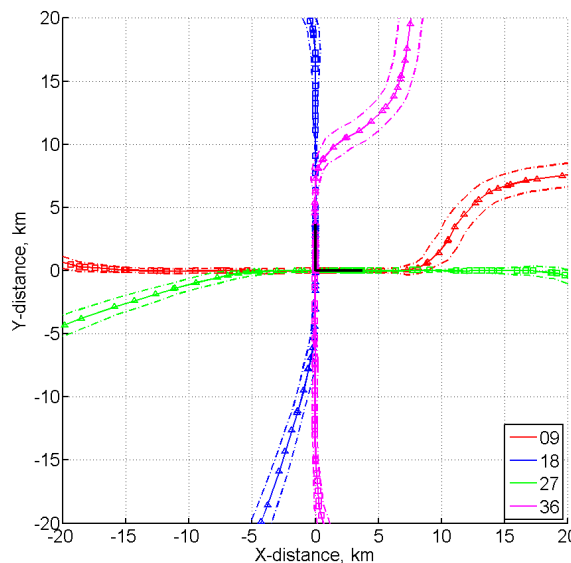

Figure 4. **The air routes from the two runways (black) in the middle of the grid. Triangles depict departure routes, the circles an approach. The dashed lines represent dispersion tracks around a main approach/departure route whereas the colors indicate a specific runway that is used.**

For ease of comparison, a short to medium range (single-aisle) aircraft is used exclusively in this study together with an according NPD table for the noise levels. The corresponding A-weighted reference spectrum is shown in the appendix as Figure 9. Due to the difference in required thrust levels between approach and departure procedures, the spectra are also different. Since atmospheric absorption is frequency dependent, the atmosphere will have a different impact on both spectra as they travel through the atmosphere before reaching the ground.

D. Atmospheric variations and effective flights

A common limitation for this type of research is the availability of weather data at different altitudes for the entire year. For this study, data is taken from a balloon sounding station in the Netherlands where twice a day, at noon and midnight, a sounding of the atmosphere is executed. The results of a balloon sounding include temperature, humidity, wind direction and wind speed for a variety of altitudes and can be accessed through the internet.[20] The current simulation uses data for 2010 which amounts to a total of 730 balloon sounding files. Further analysis showed that 6 out of the 730 files contained invalid atmospheric data, i.e. empty wind, temperature, or humidity entries, and were therefore excluded. Figure 10, included in the appendix for brevity, shows the mean of the resulting atmospheric conditions as used in this study.

Due to the availability of two sounding files per day it is possible to simulate the atmospheric impact on two time instances. However, it is not possible to calculate individual aircraft departing or approaching during the day. To circumvent this, each sounding file is used for 200 effective flights evenly distributed over the approaches and departures. The number of effective flights (N_e) is defined according to:

$$N_e = \Gamma \cdot N \cdot \sum_{i=1}^{3} T_i \tag{3}$$

where, Γ is the period-of-day multiplier associated with the L_{DEN}, N is the amount of operations during that period and T_i is the traffic load over the main and dispersed ground trajectories. For example, a traffic load T_i for the main route of 0.6 and 0.2 for each sub route and a day event (when Γ is 1), 200 operations are needed to model 200 effective flights. If the period-of-day is changed to a night event, Γ becomes 10, which equates to 20 operations. The use of effective flights allows a representative comparison of the results associated with each sounding file combined with a specific route. By using 400 effective flights per day, the amount of traffic and L_{DEN} will resemble values found around mid-size airports.

While in reality the atmosphere will change from flight to flight, we are interested in the large variations in the atmosphere and the effects on the yearly contour. This effect is still captured by combining the sounding files with the effective flights.

III.   Results

Results of the study are presented as noise contours for the 58 L_{DEN} and 48 L_{DEN} values. In this case, since no specific evening flights are modeled, these values are equivalent to L_{DN} values. The contour values are typical for noise policy related questions in the Netherlands. Since noise values are higher when the aircraft is near the ground, close to the airport, the inner contours always represent the 58 L_{DEN} value whereas the outer contours are the 48 L_{DEN}. This hold for all the contour plots shown in this paper.

Three different options are studied here:

1. Default
2. Default + Atmospheric Absorption (AA)
3. Ray tracing solution

Option 1 is the most basic setting of the noise model and includes the default, empirical LA. Option 2 is the same as option 1 but corrects for a non-standard atmosphere by correction of the difference in atmospheric absorption which is assumed to be uniform (ground level values for humidity and temperature) through the atmosphere. Option 3 is the ray tracing based calculation of the EA. Figure 5 shows the 58 and 48 L_{DEN} contours for 2010 using the three modeling options.
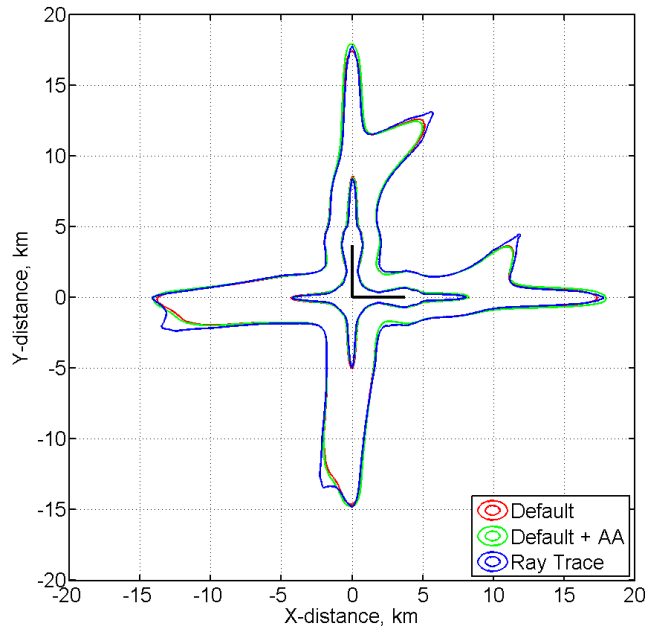
Figure 5. **The LDEN contours for 2010. The outer contour reflects the 48 LDEN and the inner contour the 58 LDEN.**

From Figure 5 it becomes clear that the contours are only slightly different. At first sight, it seems that only the 48 L_{DEN} (outer) contours shows noticeable differences between the modeling options. Since the contours, predicted by the different options, do not exhibit major differences, it further strengthens our trust in the ray tracing as it provides comparable results to the underlying empirical EA corrections. To compare the contours to each other more precise, a comparison can be made based on the area enclosed by such a contour. This area is calculated and the results are listed in Table 1.

Table 1. **The area of the 58 and 48 LDEN contours for 2010.**

Method	58 LDEN area, km^2	48 LDEN area, km^2
Default	21.1	166.9
Default + AA	20.6	171.7
Ray Tracing	18.1	175.0

Monthly contour results for the year 2010 are shown in Figure 11 which is included in the appendix for the sake of brevity. These contours change from month to month due to the different wind directions on the ground. Depending on the wind direction, the specific approach or departure routes and runways are selected. For instance, from January until March there are not many occasions that the wind is coming from the North (see Figure 10). However, from April until June a North wind is often present. As a result, the departures to the North (see Figure 4) are flown more often and the contour grows in that particular area. By calculating the enclosed area of the contours it is possible to get an impression how the contours change. Figure 6 shows the contour area for both the 58 and 48 L_{DEN} on a monthly basis.
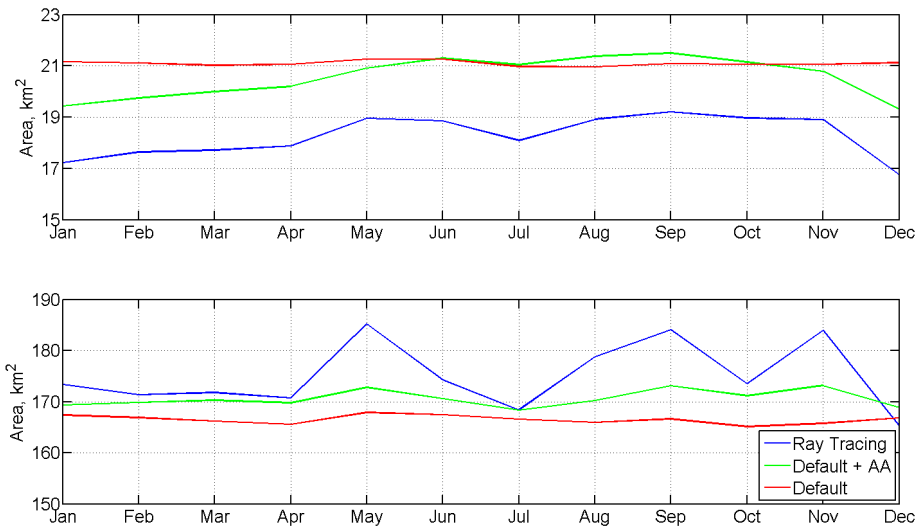
Figure 6.   The top picture shows the enclosed area of the 58 LDEN contour, the bottom plot shows the 48 LDEN area.

Based on these results, four main observations are made that are further elaborated in the discussion section that follows.

A. The large differences found for single-event results (Figure 3) are not present in the yearly contours.
B. The contour area of the 58 L_{DEN} predicted by ray tracing is always smaller than the area calculated using the default and the corrected default method.
C. A similar variation (or trend) is visible in the ray tracing result and the corrected default method, especially for the 58 L_{DEN}.
D. Peaks occur in the 48 L_{DEN} contour area line, predicted by ray tracing, in the months May, September and November.

IV. Discussion

The observations made in the results section are treated next. Please note that observation A is related, for a large part, to refraction of sound. Observation B is judged to be caused by the ground reflection model whereas observations C and D are hypothesized to be related to atmospheric absorption.

A. Wind effects on contour

The difference between Figure 3 and Figure 5 is clearly noticeable. The single-event results are influenced a lot more by the prevailing wind compared to the multi-event calculation. For the considered atmospheric input of the multi-event calculation, there is no clear prevailing wind although the South-West direction seems to be the most likely candidate upon inspection of Figure 10. Since the multi-event results are based on multiple single-events, the associated effects of Figure 3 are inherently included in the calculation. The yearly contours do not show striking differences between the modeling options. This confirms that refractive propagation effects average out when considering multi-event calculations for the used atmospheric data.

Only when zoomed in on a monthly contour small differences, which can be linked to refraction, become noticeable. Figure 7 shows such an enlarged result for the month June of which the original size picture can be found in Figure 11.
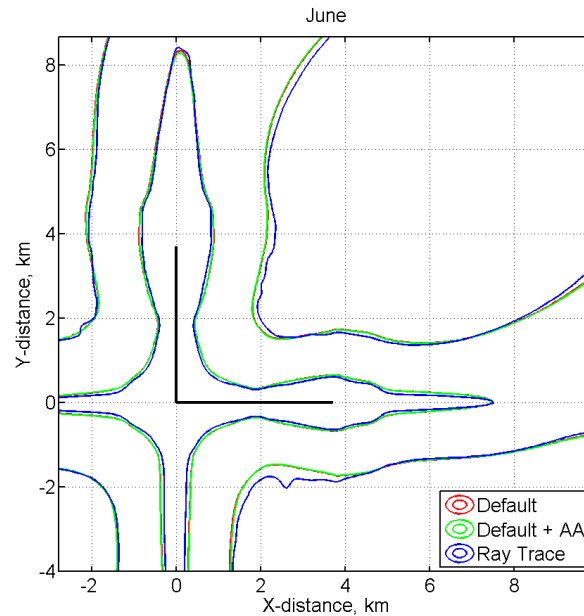
12

Figure 7.   An example of an enlarged contour of June.

If the 48 L_{DEN} contour in Figure 7 is examined in the North direction, at a Y-distance of 4 kilometers, it is seen that the blue ray tracing result shifts slightly to the East. A similar observation is made, although the effect is less prominent, on the East part of the contour. At distances further away from the runways the absorption effects, which are omni-directional unlike wind, start to dominate. Consequently, these observations are only made for contours relatively close to the runway. Note that as long as a contour shifts, the contour area does not change and therefore cannot explain the differences encountered in Figure 6. The shifting effect on the 48 L_{DEN} contour does not occur as prominently in an enlarged example of the yearly contour which is, for that reason, not included here.

Another wind effect is the irregular North-East and South-East corner of the blue 48 L_{DEN} contour lines near the airport predicted by ray tracing. Differences on the 48 L_{DEN} contour due to the wind thus only occur near the runway and the most noticeable increase in contour area is in between the two runways. It is also noted that these deviations occur around an angle of 45 degree from a particular runway. This corresponds to maximum cross-wind direction. If the cross-wind angle would be more than 45 degree, the approach or departure is executed on a different runway. The wind effect is thus emphasized at the maximum cross-wind direction. These positions are close by the runway and thus influenced when the aircraft is flying relatively low. This is a favorable condition for refractive propagation effects to occur. On the overall yearly 48 L_{DEN} contour this effect is still noticeable albeit small as the contour area is increased by approximately 1 sq. km.

B. Smaller 58 L_{DEN} contour due to ground reflection

Considering Figure 7, it is observed that the 58 L_{DEN} contour, calculated with ray tracing, shows a small constant offset everywhere compared to the green line. This constant offset, when integrated into an enclosed contour area, becomes the constant difference between the green and blue line in Figure 6.

Given the small propagation distances, where refractive effects are small, the difference between the 58 L_{DEN} contours is influenced by the varying absorption or the ground model. Whereas the atmospheric absorption will vary for each sounding file, the ground attenuation is not influenced by the atmospheric variation. The ground model is tuned to be zero directly underneath the flight path to represent the measurement conditions for NPD tables, as mentioned in section II.B. This does not exclude different results that occur at positions not directly underneath the aircraft. As such, it is hypothesized that the difference in contour area between ray tracing and the (absorption corrected) default, for the 58 L_{DEN} contour, consists out of a constant and variable component. The constant component can be associated to the ground model whereas the (smaller) variable component is due to the varying absorption.

For the 58 L_{DEN} contour, the relative distance between a route and the contour line is relatively small. As a result, the effect of variable atmospheric absorption through the atmosphere is small as well. This is reflected in a contour area variation of the absorption corrected default option of roughly 2 sq. km., visible in Figure 6. This variation is

similar to the variation in contour area as calculated with ray tracing. The remaining constant difference of roughly 2 sq. km. is attributed to the additional ground attenuation at sideline angles. The constant and variable component influencing the decrease in contour area with respect to the default are thus approximately of equivalent size.

The yearly contour shows the accumulated results of the individual months. As a result, the yearly 58 L_{DEN} contours becomes smaller when including atmospheric absorption to the default method and even smaller when selecting the ray tracing option due to the difference in ground attenuation.

C. Smaller 58 L_{DEN} contour due to absorption

The smaller yearly contour area for the 58 L_{DEN} (shown in Figure 6), is noticeable as well in the monthly contour results of Figure 11 except in the summer period ranging from May until September. In the summer months the 58 L_{DEN} contours of the three modeling options seem to coincide. When enlarged, like Figure 7, the differences appear as shown in the previous section. The differences between the three modeling options is the smallest for this period as the absorption rates are close to the standard conditions used by the default EA method.

To investigate the effect of the difference due to absorption, the difference was calculated due to the atmospheric mean conditions (see Figure 10) on the ground and at 1000 meters altitude. The results for two different months are shown in Figure 8.
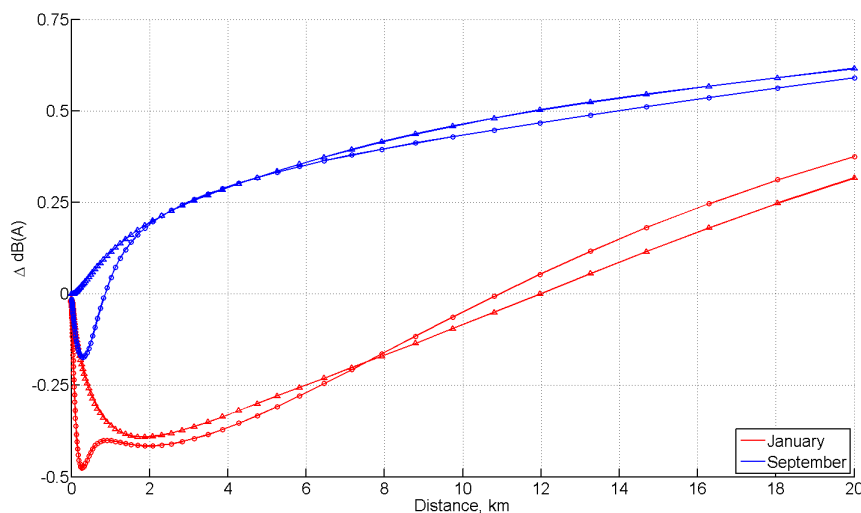

Figure 8.   The difference in absorption between the atmospheres measured on the ground and at 1000 meters. The circles depict departures whereas the triangles reflect approaches.

Figure 8 shows a few remarkable results. The dips, visible in the departure lines near the origin, are caused by the spectral shape of the departure which contains a modeled blade passage tone of 2500 Hz. More important is that the variation of humidity and temperature over altitude shows different trends for different months. Up until a distance of 12 kilometers, January shows an increased attenuation whereas at larger distances the attenuation is decreased. In September, especially in the first few kilometers, differences are smaller and more or less cancel out as the departure and approach show opposite signs in absorption. As such, September indicates that the magnitude of the remaining difference of the 58 L_{DEN} contour, caused by the ground model, is roughly 2 sq. km.

Based on the sensitivities shown in Figure 8 it becomes evident that atmospheric absorption plays a major role in the noticed contour area variation throughout the year. The differences become larger with increasing distance from the source and can exhibit opposite trends between different months.

D. Peaks in the 48 L_{DEN} contour area

Another remarkable effect, embedded in Figure 6, is the occurrence of peaks in the 48 L_{DEN} contour area, predicted by ray tracing, in the months May, September and November compared to the other months. Upon close inspection of the atmospheric data (Figure 10), specifically the relative humidity, a more or less similar pattern is found. Considering the mean relative humidity encountered in the atmosphere from 500-1000 meter, peaks occur at exactly the same months. The uppermost layer of atmosphere considered here, 1000-2000 meter, shows a similar pattern except for the month September where a peak occurs in August. On the other hand, August shows the largest contour area right behind the mentioned three months.

Although the contour area's for the 48 L_{DEN} contour are rather similar considering the yearly contour, the location of a contour plays a role as well. Especially when population densities are coupled to the contour values to calculate the amount of disturbed people. In Figure 5 it is noted that the ray tracing contour lines (blue) sometimes predict a local increment in contour size compared to the default (red) lines whereas the corrected default (green) show a slight decrease. Using the default correction thus sometimes gives an erroneous indication where a contour can grow or shrink due to varying atmospheric absorption.

In general, the deviations between the default and the ray tracing method are, for the 48 L_{DEN} contour, largest below the departure route. The contour does not deviate as much underneath the approach routes. There are two prominent differences between the two that cause these deviations: the altitude and the source spectrum. During take-off, the aircraft flies a route that quickly gains altitude whereas in approach the aircraft descends gradually from an already relatively low altitude. A difference in altitude causes a longer acoustic ray path through layers of atmosphere described by varying humidity and temperature properties. In case of ray tracing, these effects are accumulated over the path and therefore taken into account. Given the longer propagation path in a departure, the associated differences in absorption from Figure 8 are accentuated compared to the shorter propagation distances in approach. This is magnified by the difference in the source spectrum that is associated with the difference in thrust level used throughout the departure or approach. Absorption differences tend to increase with higher frequencies which are commonly present in the departure spectrum. The combination of higher altitude and source spectrum make that the contours, calculated by the different models, vary most underneath the departure route.

V. Conclusion

In order to assess the effects of a varying atmosphere, the Doc.29 noise model implemented at NLR has been updated. The update consisted of supplying the noise model with an augmented ray tracing solution to predict the EA rather than using an empirical model. The underlying core model, supplemented by the ray tracing, showed similar calculation times. As a result, it is thus attractive for studies that require a lot of runs like noise driven trajectory optimization and yearly contour calculations.

The impact of wind on results predicted for a single aircraft operation can be large. These effects cannot be predicted by the empirical EA models. The empirical model, based on measurements, is averaged out over long terms and thus reflects a solution for a similar period. To compare the ability of the empirical model to a more theoretical propagation model, it was compared to solutions for an entire year. This comparison helps to answer the two main research questions stated in the introduction.

First the influence of varying weather on the L_{DEN} contour is treated or, in other words, the first research question is answered. The 58 L_{DEN} and 48 L_{DEN} contours are affected differently, compared to the default EA method, when ray tracing is applied to the varying atmospheric conditions. The 58 L_{DEN} contour area decreases whereas the 48 L_{DEN} contour area increases. This observation is made while comparing the default to both the corrected default and ray tracing options. Wind effects translate the contour slightly and cause small irregular contour lines in the corners of the 48 L_{DEN} contour. The added area to the yearly contour due to this effect is in the order of 1 square kilometer. This effect only occurs on the 48 L_{DEN} contour as propagation effects are more prominent at larger distances. No wind effects were distinguished for the 58 L_{DEN} contour. As such, the decrease in 58 L_{DEN} contour area is believed to be caused by the ground attenuation and the varying absorption. The difference due to the ground attenuation is constant throughout the year whereas the absorption may vary. Both components are, in this case, of approximately equal size.

The yearly contour indicates that the major differences can be expected underneath the departure route for the 48 L_{DEN} contour. It is argued that this is caused by the combination of the departure source spectrum and the difference in absorption encountered on the ray path traveling through the varying atmosphere.

The second research question inquired if the standard correction method is representative for a varying condition for an entire year. This default empirical model is, compared to the ray tracing solution, certainly applicable to calculate a yearly average since the difference in contour area is small. The absolute difference in contour area can be improved by including the default correction for atmospheric absorption as calculated on the ground. Although this must be treated carefully as contours may sometimes grow at a specific location whereas the corrected default predicts a shrinking contour. Differences due to absorption logically increase when the aircraft is flying at relative high altitudes when sound waves travel through, possibly, varying absorption layers due to atmospheric differences. Wind effects can be distinguished from a yearly contour but are or minor importance compared to the varying absorption.

The stated conclusions only hold for the considered atmosphere that is representative for the Netherlands. Other locations around the globe can have other prevailing winds, humidity and/or temperature conditions which may influence a contour calculation. Further research would therefore be necessary to generalize such a conclusion for other airport locations. Different aircraft may also be more susceptible to these effects as they climb slower or faster than the used aircraft.

To isolate the effect of wind, a separate calculation with variable absorption over a straight-line path is considered in the future for comparison to the found contours. This will ultimately answer whether treating the variable absorption along a straight ray path is the most important effect for an EA model. From that point it is possible to investigate if a more theoretical EA model without wind effects is viable and gives comparable results if only ground surface impedance and varying absorption effects are included.
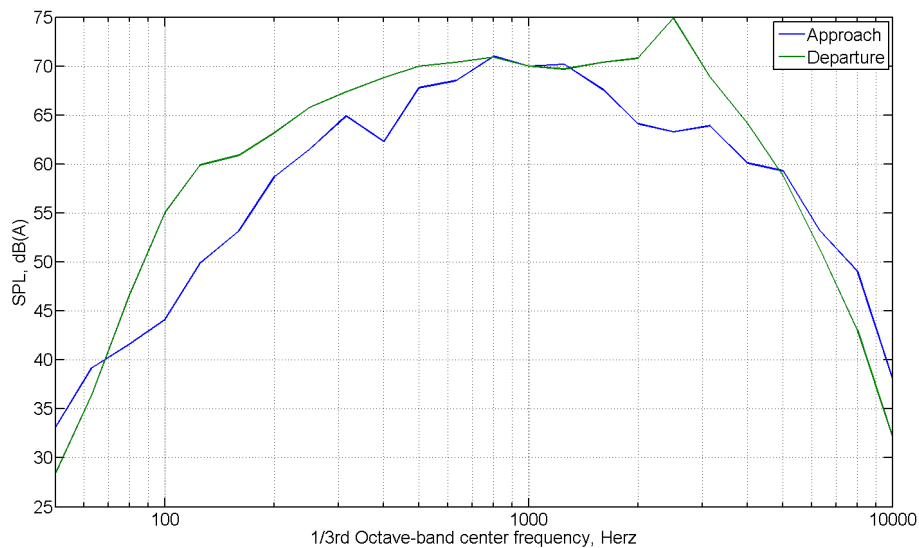
Appendix

Figure 9.   The normalized representative spectra of the used short to medium range (single-aisle) aircraft equipped with CFM56-7B engines. The spectrum is propagated to a reference distance of 1000 ft. using a standard absorption rate.[5]
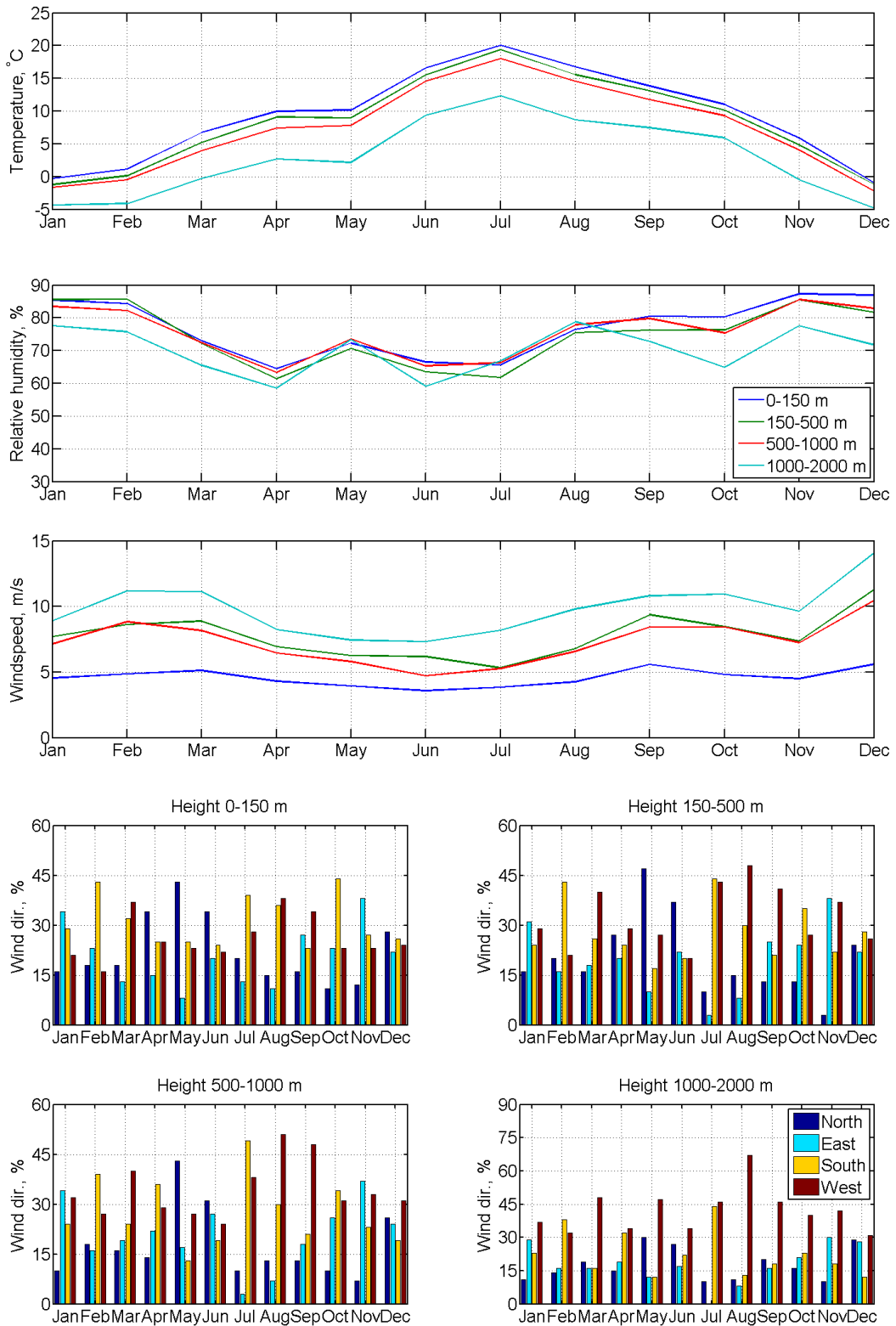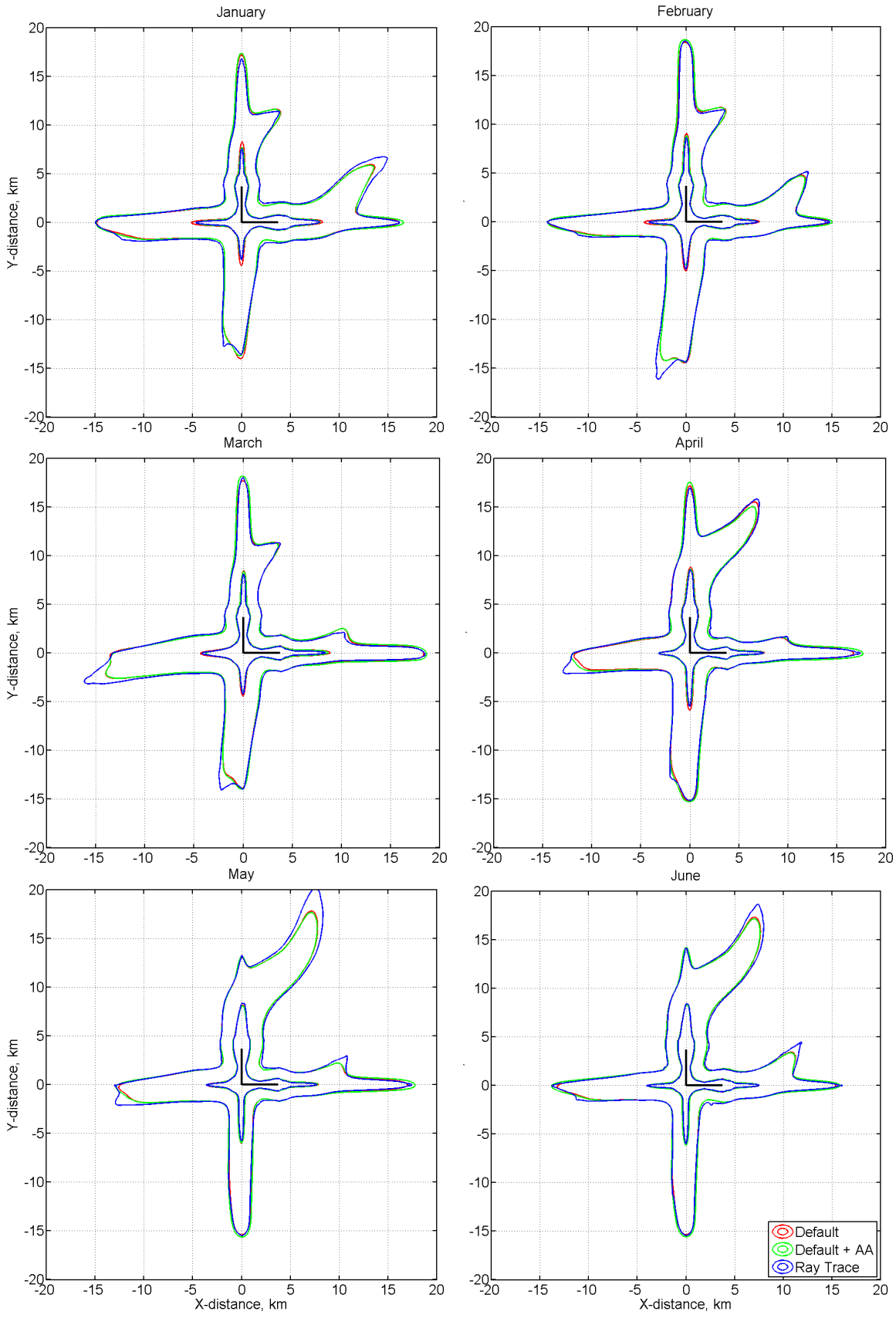
Figure 10. The mean atmospheric conditions as used in this study. Please notice that the results are presented for different altitudes and combine both day and night events. The wind (from) direction results are presented as a percentage, i.e. the wind is blowing from a direction for a percentage of the combined results during the month.
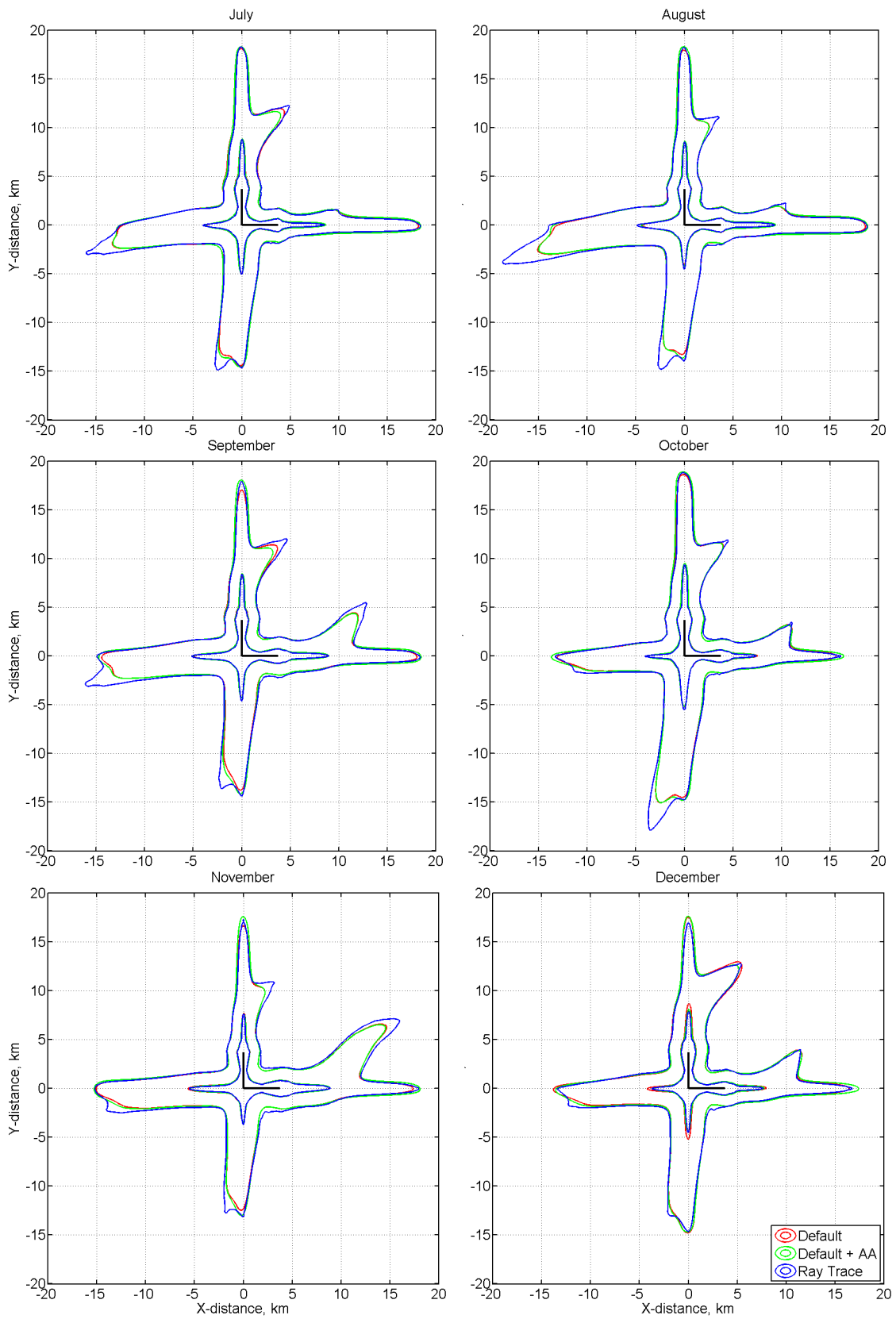
Figure 11. Monthly contour plots for 2010.

Acknowledgments

References

1. http://www.boeing.com/commercial/cmo/, visited 27-07-2012.

2. http://www.airbus.com/company/market/forecast/passenger-aircraft-market-forecast/, visited 27-07-2012.

3. Integrated Noise Model (INM) Version 7.0 Technical Manual, FAA-AEE-08-01, January 2008

4. Report on Standard Method of Computing Noise Contours around Civil Airports, ECAC.CEAC Doc.29, 3rd Edition, Volume I, December 2005

5. Report on Standard Method of Computing Noise Contours around Civil Airports, ECAC.CEAC Doc.29, 3rd Edition, Volume II, December 2005

6. Next generation aircraft noise models – need and requirements, Granøien I.L.N, Randeberg R.T., Olsen H, InterNoise, 13-16 June 2010, Lisbon, Portugal.

7. Effects of atmospheric absorption on aircraft noise propagation during takeoff and landing around airports in the various world regions, Okada Y., Yoshihisa K., Iwase T., InterNoise, 13-16 June 2010, Lisbon, Portugal.

8. Method for Predicting Lateral Attenuation of Airplane Noise, SAE-AIR-5662, April 2006

9. A weather dependent noise contour prediction concept: Combining a standard method with ray tracing, S.J. Hebly, M. Arntzen, D.G. Simons, In proceedings of EuroNoise 2012, pp. 405-410, 11-13 June 2012, Prague

10. A framework for simulation of aircraft flyover noise through a non-standard atmosphere, M. Arntzen, S.A. Rizzi, H.G. Visser, D.G. Simons, 18th Aeroacoustics AIAA/CEAS Aeroacoustics conference, AIAA 2012-2079, 4-6 June 2012, Colorado Springs CO, USA.

11. Propagation Effects of Wind and Temperature on Acoustic Ground Contour Levels, S.L. Heath and G.L. McAninch, in proceedings of the 44th AIAA Aerospace Sciences Meeting and Exhibit, 2006

12. Aircraft Noise Impact Under Diverse Weather Conditions, J. Huber, J-P.B. Clarke and S. Maloney, in proceedings of 9th AIAA/CEAS AeroAcoustics Conference and Exhibit, 2003

13. Computational Atmospheric Acoustics, E.M. Salomons, Kluwer Academic Publishers, 2001

14. Elements of aviation acoustics, G.J.J. Ruijgrok, VSSD, Delft, 2007.

15. An introduction to ray tracing. Academic press limited, A. S. Glassner., 3rd edition, 1990.

16. Prediction of sound attenuation in a refracting turbulent atmosphere with a Fast Field Program, anon., ESDU 04011, May 2004.

17. Acoustical properties of fibrous absorbent materials, M. E. Delany, and E. N. Bazley, Applied Acoustics 3, 105-116, 1970

18. Procedure for the computation of airplane noise in the vicinity of airports, Society of Automotive Engineers, Committee A-21, SAE AIR 1845, Warrendale, PA: March 1986.

19. Standard values of atmospheric absorption as a function of temperature and humidity, Society of Automotive Engineers, Committee A-21, SAE AIR 866A, Warrendale, PA: March 1975.

20. http://weather.uwyo.edu/upperair/sounding.html, visited 24-07-2012.